

Optical, Structural and Morphological Properties of Photocatalytic ZnO Thin Films Deposited by Pray Pyrolysis Technique

Durgam Komaraiah, Eppa Radha, Y. Vijayakumar, J. Sivakumar, M. V. Ramana Reddy, R. Sayanna

Department of Physics, University College of Science, Osmania University, Hyderabad, India

Email: dkumarou@gmail.com

How to cite this paper: Komaraiah, D., Radha, E., Vijayakumar, Y., Sivakumar, J., Reddy, M.V.R. and Sayanna, R. (2016) Optical, Structural and Morphological Properties of Photocatalytic ZnO Thin Films Deposited by Pray Pyrolysis Technique. *Modern Research in Catalysis*, 5, 130-146. <http://dx.doi.org/10.4236/mrc.2016.54011>

Received: September 10, 2016

Accepted: October 18, 2016

Published: October 21, 2016

Copyright © 2016 by authors and Scientific Research Publishing Inc.

This work is licensed under the Creative Commons Attribution International License (CC BY 4.0).

<http://creativecommons.org/licenses/by/4.0/>



Open Access

Abstract

Photocatalytic ZnO thin films have been deposited onto glass substrate by spray pyrolysis technique. The sprayed solution consists of 0.1 M of zinc acetate dihydrate dissolved in double distilled water and sprays onto ultrasonically cleaned glass substrates maintained at 350°C, through an air-atomizing nozzle. The X-ray diffraction (XRD), scanning electron microscopy (SEM), EDX and UV-VIS spectrophotometer were applied to describe the structural, morphological, compositional and optical properties of ZnO catalyst. XRD analysis confirms that the films were found to be single phase hexagonal wurtzite structure. The SEM micrograph of the films is shown highly uniform, crack free and found to be fiber like structures. The optical transmittance spectra of the ZnO thin films were found to be transparent to visible light and the average optical transmittance was greater than 85%. The direct optical band gap energy values of the films shift towards the lower energy as a consequence of the thermal annealing. The Urbach energy of the films was found to increase with annealing temperature. The refractive index of the films was calculated and the refractive index dispersion curve of the films obeys the single oscillator model. The values of oscillatory energy E_o , dispersion energy E_d , and static dielectric constant ϵ_s for the ZnO thin films were determined. The films were evaluated for their ability to degrade methylene blue. The Langmuir-Hinshelwood kinetic model was used to interpret quantitatively the observed kinetic experimental result. The photocatalytic activity of ZnO thin films was enhanced by annealing temperature.

Keywords

ZnO Thin Film, Spray Pyrolysis, Optical Band Gap, Refractive Index, Photo Catalysis

1. Introduction

Zinc oxide (ZnO) is an n-type semiconductor, has a hexagonal wurtzite structure, and

has been extensively studied in recent years owing to its technical importance. ZnO is widely used as a functional material because it has a direct band gap of 3.37 eV, high electron mobility, and large exciton binding energy (~60 meV) at room temperature [1]. It has excellent chemical and thermal stability, low cost, richly abundant, environment-friendly, non-toxic nature, strong oxidizing power, high photosensitivity, and high resistance to radiation damage. ZnO has now received increasing attention and recognized as a promising material because of its vast potential in many scientific and industrial areas as a micro-electronic and opto-electronic devices such as light emitting diodes [2], thin film transistors [3] [4], Varistors [5], solar cells [6] [7] [8], gas sensors [9] [10] [11] [12], and photocatalyst [13] [14]. And also, it has other applications, such as piezoelectric devices, spin based electronics or spintronics, luminescent materials, and transparent conductors [6] [8] [15] [16]. Till now ZnO thin films have been synthesized by various techniques including sol-gel spin coating method [4], low pressure chemical vapor deposition (LPCVD) [7] [8], Chemical Both Deposition (CBD) [12], spray-pyrolysis [13] [14], thermal evaporation [17], pulsed laser deposition (PLD) [18], metal organic chemical vapor deposition (MOCVD) [19], sputtering [20], molecular beam epitaxy [21], and Hydrothermal Technique [15], etc. Spray pyrolysis is widely used because of its simplicity, commercial viability, and potential for cost-effective mass production. The spray-pyrolysis technique has been successfully applied to synthesize ZnO thin films and analyzed their growing characteristics, atomic composition, surface morphology, microstructure and optical properties. Spray pyrolysis method is especially efficient in producing thin films, transparent, multi-component oxide layers of many compositions on various substrates, including glass. There are many factors affecting the physical properties of ZnO thin films, including ZnO solution concentration, solvent, substrate temperature, post deposition annealing, annealing atmosphere and film thickness. The novel results derived from this situation have encouraged the researchers to increase their interest in the field of chemically sprayed ZnO thin films. This is the reason why we focus our attention mainly on the contributions on chemically sprayed ZnO thin films.

In this article, our interest is focused on adsorption and photocatalytic ability for organic dye over ZnO catalyst in aqueous solution. We aim to synthesize promising ZnO nanofibers that behave as an efficient photocatalyst by low cost spray pyrolysis technique and effects are being made to characterize the ZnO nanofibers using structurally, morphologically and studied its photocatalytic activity.

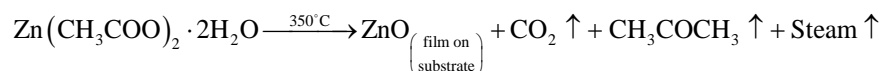
2. Experimental Details

2.1. Materials and Chemicals

Zinc acetate dihydrate [$\text{Zn}(\text{CH}_3\text{COO})_2 \cdot 2\text{H}_2\text{O}$, Himedia, 99.5%], double distilled water, methylene blue (MB), Glass micro slide substrates with dimensions 75 mm \times 25 mm \times 1.2 mm (Blue star, Polar Industrial Corporation, India) were applied for deposition of ZnO thin films by simple spray pyrolysis technique at a substrate temperature of 350°C.

2.2. Synthesis of ZnO Thin Films

The ZnO thin films were deposited on glass substrates at a substrate temperature of 350°C by spray pyrolysis deposition technique. The ZnO precursor solution was prepared by dissolving 0.1 M of zinc acetate dihydrate [Zn(CH₃COO)₂·2H₂O, Himedia, 99.5%] in 25 ml deionized water. Before deposition the glass substrates were cleaned with detergent solution, diluted HCl and deionized water. Further, ultrasonic cleaning was carried out for 30 min in an ultrasonic bath and then rinsed in acetone for 10 min. Then the ultrasonically cleaned substrates were placed on a sample holder facing the air-atomizing nozzle at a fixed distance of 28 cm in the chamber. Compressed air was used as the carrier gas at the pressure of 2 bar. The prepared solution was sprayed (3 ml/min) onto the clean glass substrates. During spray pyrolysis, a precursor solution was sprayed as fine droplets on to a heated substrate. When the droplets reach the heated substrate, they spread out and undergo pyrolytic decomposition. Finally, the solid compounds react to become a new chemical compound. The possible chemical reaction that takes place on the heated substrate to produce ZnO thin film may be as follows [22] [23].



The deposited films were annealed at 450°C for 1 hr in the muffle furnace using a ramp-rate of 10°C per minute.

2.3. Characterization

The structural properties and phase identification of the films were done by using X-ray diffractometer with CuK_α radiation ($\lambda = 1.5406 \text{ \AA}$) (Panalytical Xpert pro) for the 2θ range from 20° to 80° at room temperature. The surface morphology was studied with a scanning electron microscope (ZEISS, EVO-18). Stoichiometry of the film estimated using EDX. The UV-visible optical transmission and absorption spectra of ZnO thin films were recorded by UV-VIS spectrophotometer (UV-3092). The photocatalytic activity was evaluated by the degradation of MB under visible light irradiation and optical absorption spectrum of MB solution was measured using a UV-Vis spectrophotometer. The thickness of the film was measured by weight difference method using the relation $t = \Delta m / (g \times A)$. Where, Δm is the mass difference measured using micro balance *i.e.* mass of the substrate measured after deposition and before deposition. It is taken in grams. “A” is the surface area of the film in cm² and g is the density of deposited material (density of ZnO = 5.61 gm/cm³). The film thickness was found to be around 1.5 μm.

3. Results and Discussion

3.1. Structural Properties of the ZnO Thin Films

Figure 1, shows the phase identification and crystal structure of the ZnO thin films of the as prepared and annealed at 450°C for 1 hr. These films are found to be polycrystal-

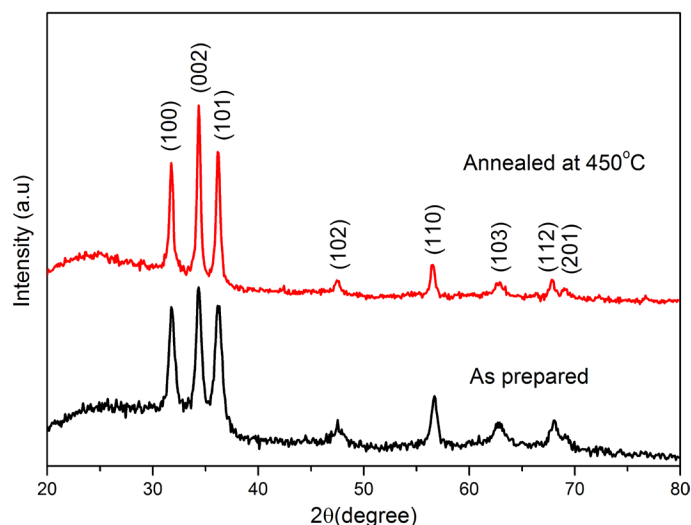


Figure 1. XRD patterns of the ZnO thin films.

line in nature and exhibit single phase hexagonal wurtzite structure. The observed XRD patterns are compared with standard JCPDS data file (File Nos. 890510). The observed 2θ values are in good agreement with the standard ones, and having a hexagonal wurtzite structure with lattice constants $a = 3.248 \text{ \AA}$ and $c = 5.205 \text{ \AA}$. It is clearly seen from the figure that the crystallinity of ZnO film increases with the annealing temperature. The films showed several diffraction peaks at $2\theta = 31.808^\circ$, 34.435° , 36.250° , 47.538° , 56.602° , 62.795° , 67.945° , and 69.120° having the inter planar spacing of 2.813 \AA , 2.605 \AA , 2.478 \AA , 1.626 \AA , 1.480 \AA , 1.379 \AA , 1.358 \AA and 1.358 \AA with orientation of (100), (002), (101), (102), (110), (103), (112), and (201) planes respectively. The ZnO thin films exhibit three prominent peaks of (100), (002), and (101) plane orientations. Again, some low intensity peaks corresponding to the orientations of (102), (110), (103), (112), and (201) are also present. The annealing temperature plays an important role on the surface reactions and species mobility. The lattice constants “ a ” and “ c ” of the hexagonal wurtzite structure of ZnO films can be calculated and was found to be $a = b = 3.252 \text{ \AA}$ and $c = 5.204 \text{ \AA}$ by using the given below relation [24].

$$\frac{1}{d_{hkl}^2} = \frac{4}{3} \left(\frac{h^2 + hk + k^2}{a^2} \right) + \frac{l^2}{c^2} \quad (1)$$

The crystallite size has been evaluated from peak profile using full width at half maximum (FWHM) of the corresponding diffraction peak using Debye-Scherrer’s formula [25].

$$D = \frac{0.9\lambda}{\beta \cos \theta} \quad (2)$$

where “ θ ” is the Bragg diffraction angle, β is the FWHM (taken in radians) of the (002) plane orientation diffraction peak and λ is the wavelength of the incident X-ray ($\lambda = 0.15406 \text{ nm}$). The lattice strain (ε) and dislocation densities (δ) were calculated using the relation given below [25].

$$\varepsilon = \frac{\beta \cos \theta}{4} \quad (3)$$

$$\delta = \frac{1}{D^2} \quad (4)$$

The dislocation density (δ), defined as the length of dislocation lines per unit volume of the crystal and it gives more information about the crystal structure. Better the crystallization smaller will be the dislocation density. The crystallite size found to increase with increase in annealing temperature, whereas the strain and dislocation density are found to decrease.

The preferential growth orientation was determined using a texture coefficient $TC(hkl)$. This factor can be calculated using the following relation [26].

$$TC_{hkl} = \frac{I(hkl)/(I_s hkl)}{n^{-1} \sum_n I(hkl)/(I_s hkl)} \quad (5)$$

where $TC(hkl)$ is texture coefficient, $I(hkl)$ is the measured XRD intensity of a plane (hkl) obtained from the films, $I_s(hkl)$ is the standard intensity of the plane (hkl) taken from the JCPDS data, and n is the number of diffraction peaks considered. The variations of texture coefficient calculated for the three main diffraction peaks ((100), (002) and (101)) of wurtzite ZnO, are listed in **Table 1**. The texture coefficient for the (002) orientation has been found to increase from 1.476 to 1.622 with annealing temperature. The value of the texture coefficient indicates a sample with randomly oriented crystallite presents $TC(h, k, l) = 1$, while the larger value, the larger abundance of crystallites oriented at the (hkl) direction. Thus, in the present investigation, with increase in annealing temperature, the crystallinity along (002) plane improves.

3.2. Surface Morphology and Composition Analysis of ZnO Thin Films

Figure 2, shows the surface morphology of as deposited and annealed ZnO thin films. SEM micrographs reveals that the thin films were found to be crack free, having uniform texture the substrate and the films were found to be nano fiber like structure. The average diameter of the fibers for the as deposited and annealed at 450°C was found to be approximately 390 nm, and 400 nm respectively. Ilican *et al.* (2006) also reported the indium-doped zinc oxide nanofibers with uniform diameter of 200 nm [26]. In our investigation the average diameter of the fibers increases with annealing temperature, this is probably due to agglomeration during annealing process, and producing thicker

Table 1. Microstructural parameters of ZnO thin film.

Sample	TC (100)	TC (002)	TC (101)	FWHM (β) (deg)	Crystallite size (D) (nm)	Lattice strain ϵ (10^{-3})	Dislocation density (δ) $\times 10^{-3}$ (nm^{-2})
As prepared	0.968	1.476	0.556	0.5377	15.46	2.24	4.184
Annealed at 450°C	0.855	1.622	0.524	0.3418	24.23	1.42	1.691

TC is the texture coefficient; FWHM is the full width at half maximum.

diameter of fibers. Similarly it has been observed that the annealing temperature has profound influence on the diameter of the nano fibres [27]. Stoichiometry and Compositional analysis of ZnO thin film was carried out by the energy dispersive X-ray spectrometer (EDX) shown in **Figure 3**. The EDX analysis confirmed the presence of Zn and O elements in the ZnO film.

3.3. Optical Studies

The optical properties of bulk materials and thin films that are very important for optoelectronic applications, the properties include absorbance (A), transmittance (T), and reflectance (R), which characterize the interaction of incident radiation with a particular coating of material. These properties are also related to intrinsic properties of films such as coefficient of absorption (α), extinction coefficient (k), refractive index (n),

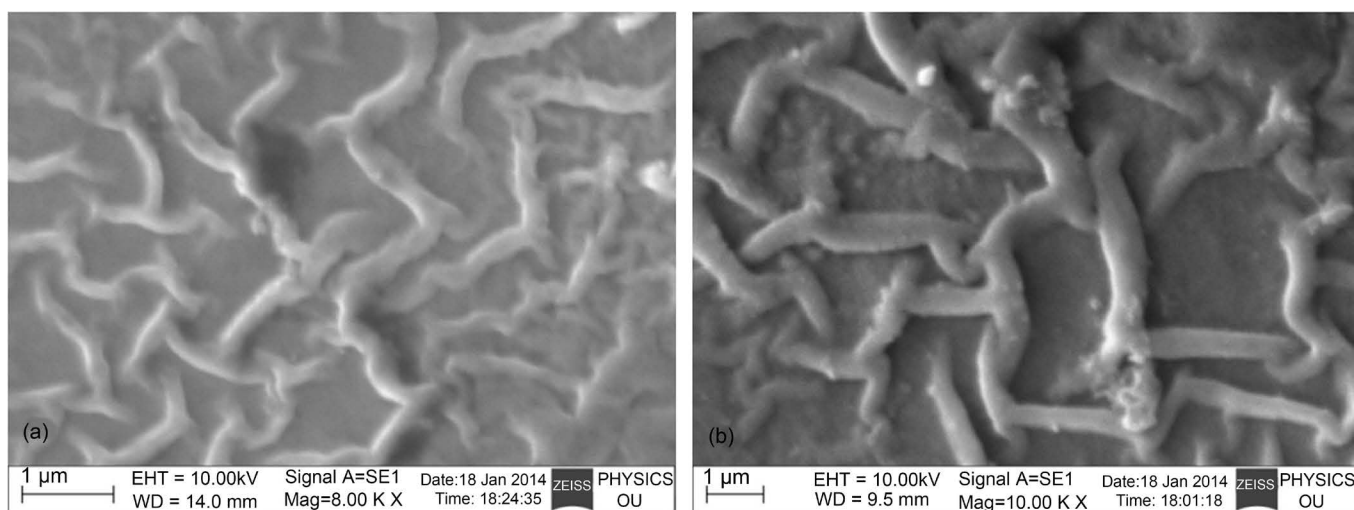


Figure 2. SEM images of ZnO thin films: (a) as deposited, (b) annealed at 450°C.

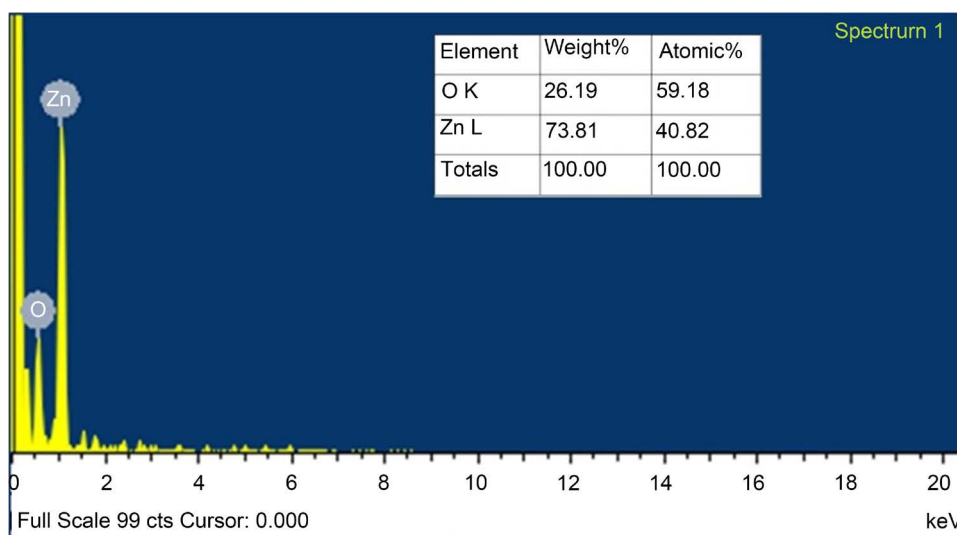


Figure 3. EDX analysis of ZnO thin film annealed at 450°C.

band gap energy and optical conductivity. In the present investigation, we calculated the absorbance and transmittance as a function of the wave length at room temperature. From the above parameters the reflectance of the films can be estimated using the following relation [28].

$$A + T + R = 1 \quad (6)$$

The optical transmittance and absorbance of ZnO films of as prepared and annealed at different temperatures shown in **Figure 4(a)** and **Figure 4(b)**. Absorption spectrum indicates that the absorption of light in visible region is very low and greater in the UV region. Absorption spectra of ZnO thin film shows that the absorption edge is slightly moved towards longer wavelength side (red shift) with increase in annealing temperature

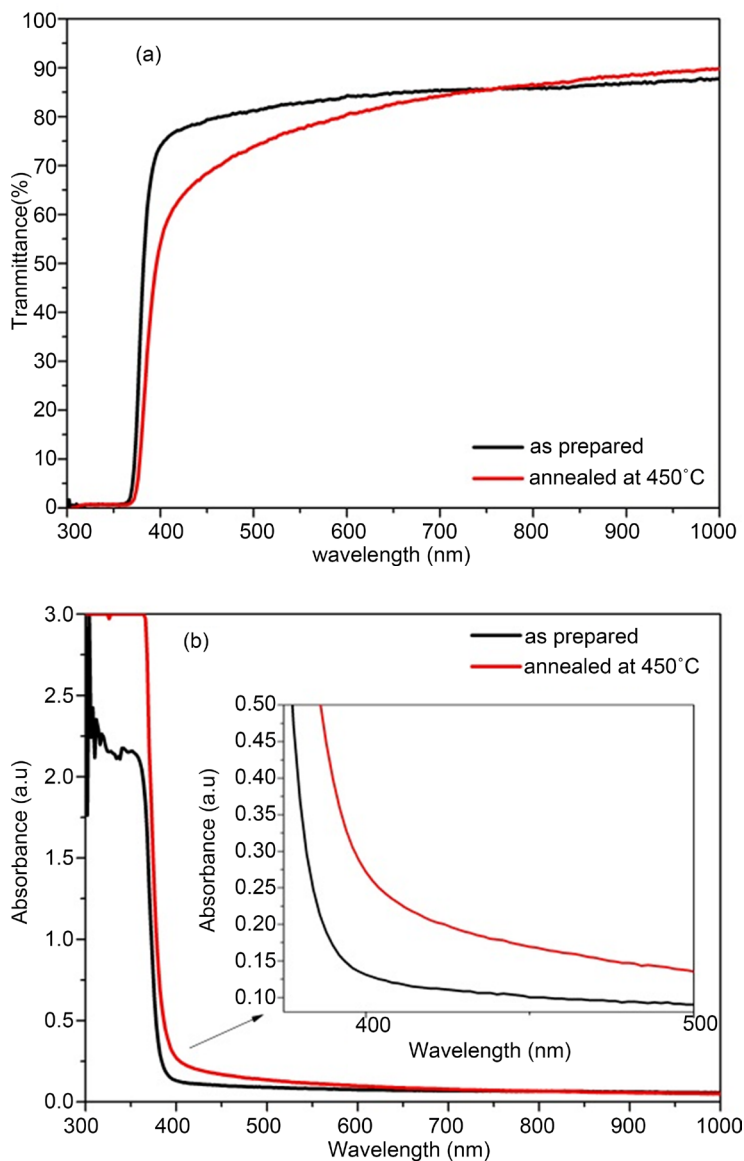


Figure 4. (a) Optical transmittance spectra of ZnO thin films, (b) Optical absorption spectra of ZnO thin films.

due to the change in band gap of ZnO thin film due to change in crystallite size. ZnO film exhibits high transmittance (>85%) in the visible region, the transmission of ZnO film is high over large wavelengths. This suggests that the produced film indicates a good optical quality due to the low scattering/ absorption losses. In nanocrystalline semiconductors, the following equation has been obtained to relate the absorption coefficient to incident photon energy $h\nu$. The absorption coefficient $\alpha(\lambda)$ has been calculated using Lambert's law [29] [30]

$$\alpha(\lambda) = \frac{\ln(1/T)}{t} \quad (7)$$

where t is the thickness of film. The extinction coefficient can be obtained from the relation $k = \frac{\lambda\alpha}{4\pi}$, where λ is the wavelength of the incident radiation impinging on the film. The extinction coefficient as a function of wavelength and it is observed that the extinction coefficient decreases with the increase of annealing temperature. This behavior of the absorption coefficient $\alpha(\lambda)$ and the extinction coefficient (k) is similar to the optical absorption behavior. The Optical energy gap E_g and absorption coefficient $\alpha(\lambda)$ are related by the equation [29] [30]

$$\alpha(\lambda)h\nu = B(h\nu - E_g)^r \quad (8)$$

where $h\nu$ is the photon energy, $\alpha(\lambda)$ is the absorption coefficient, E_g is the optical band gap and B is the slope of the tauc edge, called the band tailing parameter and the exponent " r " depends on the type of optical transition, which is 1/2 for direct allowed transition and 2 for indirect allowed transition. Whether the film has direct or indirect band gaps will be determined from the linearity of the plots of $(\alpha h\nu)^2$ versus $(h\nu)$ and $(\alpha h\nu)^{1/2}$ versus $(h\nu)$ respectively. **Figure 5**, shows the tauc plots of ZnO thin films. The band gap values have been calculated by extrapolating the straight line portion of the curve of $(\alpha h\nu)^2$ against $(h\nu)$ to meet the x-axis. The band gap of the ZnO film was obtained as a direct band gap by the optical method, which was described above. **Table 2** gives the values of E_g of the ZnO thin films of as deposited and annealed at different temperatures. The band gap energy of the films was found to decrease with increase of annealing temperature. The change in the values of band gap energy may attribute to a decrease of the optical band gap due to interatomic distances with increasing annealing temperature on ZnO film [20]. The tail of the absorption edge is exponential, it indicates the presence of localized states in the band gap energy. The absorption edge gives a measure of the band gap energy and the exponential dependence of absorption coefficient $\alpha(\lambda)$ on photon energy near the band edge for many materials. This dependence is given by Urbach F., 1953 [31].

$$\alpha(\lambda) = \alpha_o \exp\left(\frac{h\nu}{E_u}\right) \quad (9)$$

where α_o is a constant and E_u is Urbach energy, which is the width of the tail of the localized states corresponding to the optical transition between localized states adjacent to the valence band and extended state in the conduction band which is lying above the

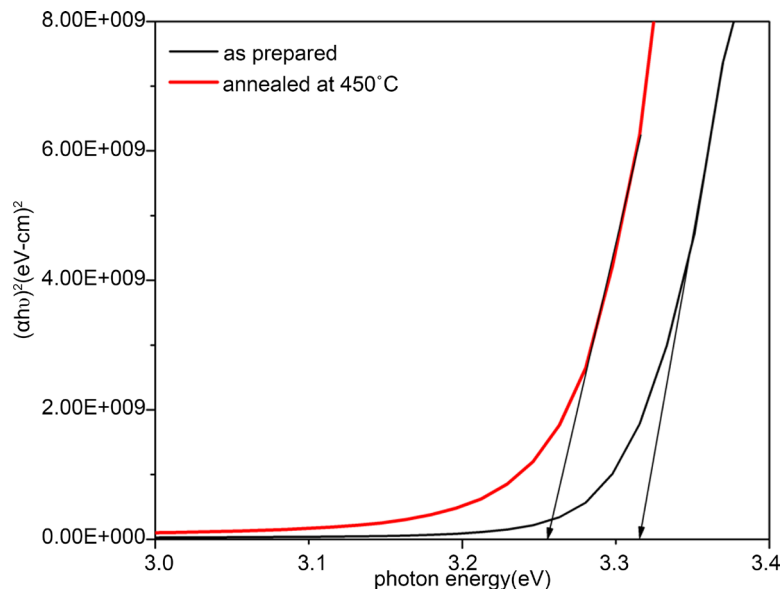


Figure 5. Plots of $(ah\nu)^2$ versus photon energy $(h\nu)$ of ZnO thin films.

Table 2. Optical parameters of the ZnO thin film.

Sample	E_g (eV)	E_u (meV)	E_o (eV)	E_o/E_s	E_d (eV)	M_{-1}	M_{-3} (eV) ⁻²	ϵ_s	λ_o (nm)	n_o	$S_o \times 10^{13}$ (m) ⁻²
As prepared	3.31	75.75	6.62	2.00	12.49	1.887	0.043	2.89	269	1.69	2.57
Annealed at 450°C	3.26	95.27	6.04	1.85	12.38	2.05	0.056	3.05	323	1.75	1.96

E_g is the band gap energy, E_u is the Urbach energy, E_o is the oscillatory energy, E_d is the dispersion energy, M_{-1} and M_{-3} are the moments; ϵ_s is the static dielectric constant, λ_o is the oscillator wavelength, S_o is the oscillator length strength.

mobility edge. The plot of $\ln\alpha$ vs. photon energy $(h\nu)$ plots for ZnO thin films of is shown in **Figure 6**. The values of E_u , were obtained by taking the reciprocal of the slope of the linear region of the plots of $\ln\alpha$ versus $(h\nu)$ and are listed in **Table 2**. In our observation, the increase in Urbach energy may be attributed to the increase of thermal induced structural disorder of the film within this temperature range.

Figure 7, shows the plot of refractive index (n) versus wavelength (nm) of ZnO thin films and it indicates that the refractive index decreases with increase in wavelength. Refractive index of the films was calculated from the following relation [32].

$$n = \frac{1+R}{1-R} + \sqrt{\left(\frac{1+R}{1-R}\right)^2 - (k^2 + 1)} \tag{10}$$

where R is reflectance and k is extinction coefficient. The refractive index dispersion of the ZnO films studied can be fitted by the single-oscillator model (described by Wemple and DiDomenico, 1971). The dispersion plays an important role in the research of optical materials, because it is a significant factor in optical communication and in designing devices for spectral dispersion. The result of refractive index dispersion below

the inter band absorption edge corresponds to the fundamental electronic excitation spectrum, according to the Wemple-DiDomenico single oscillator model, the refractive index is related to photon energy through the relationship [33] [34].

$$n^2(h\nu) - 1 = \frac{E_o E_d}{E_o^2 - (h\nu)^2} \tag{11}$$

where E_o and E_d are single-oscillator parameters. Values of E_o and E_d can be determined from the slope ($1/E_o E_d$) and intercept (E_o/E_d) on vertical axis of the curves of $(n^2 - 1)^{-1}$ vs. $(h\nu)^2$ by fitting a linear function to the smaller energy data shown

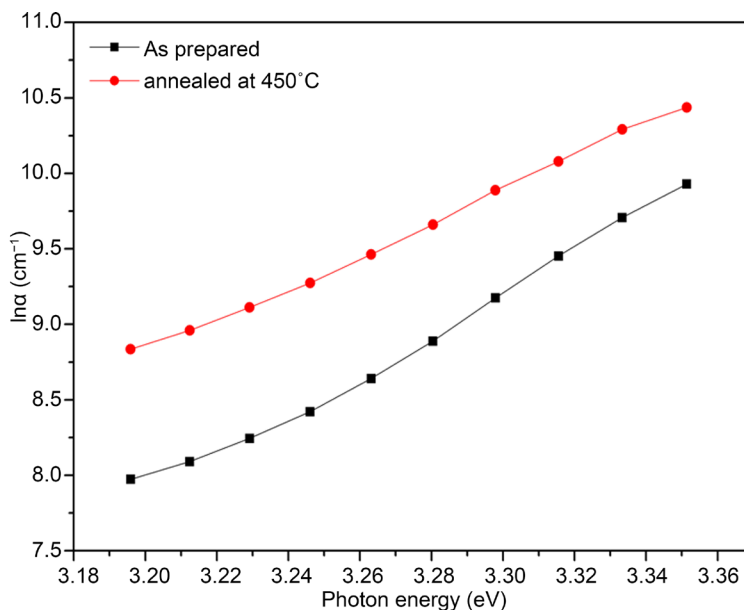


Figure 6. Plots of $\ln \alpha$ versus photon energy ($h\nu$) of ZnO thin films.

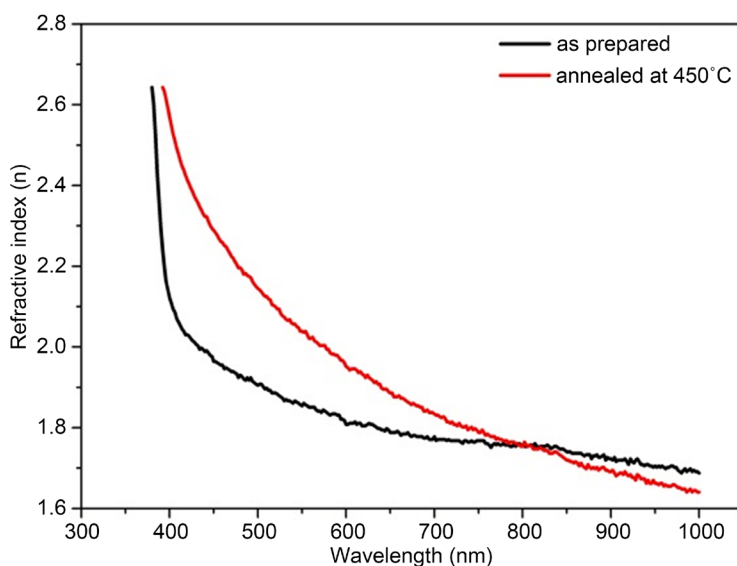


Figure 7. The refractive index plots of ZnO thin films.

In **Figure 8** and they are given in **Table 2**. The oscillator energy E_o is average excitation energy for electronic transitions. The dispersion energy E_d which is measure of the average strength of inter band optical transitions or the oscillator strength are single oscillator parameters. We found that the E_o values of the deposited film is related empirically to the lowest direct band gap by $E_o \approx 2E_g$. E_o values decreased with an increase in annealing temperature. According to the single-oscillator model, the single oscillator parameters E_o and E_d are related to the imaginary part of the complex dielectric constant. The static (zero frequency) refractive index $n(0) = (1 + E_d/E_o)^{1/2}$ and the static dielectric constant ($\epsilon_s = n^2(0)$) were calculated using Equation (11). The calculated values of the oscillator energies (E_o), the dispersion energies (E_d), and ϵ_s for the ZnO thin film are summarized in **Table 2**. The refractive index is represented by a single Sellmeier oscillator at low energies and the refractive index was also analyzed to determine the long wavelength refractive index (n_∞), average inter band oscillator wavelength (λ_o) and the average oscillator length strength (S_o) parameters, for the ZnO thin films. These parameters can be determined by using the following equation [35].

$$\frac{(n_\infty^2 - 1)}{(n^2 - 1)} = 1 - \left(\frac{\lambda_o}{\lambda}\right)^2 \tag{12}$$

where (n_∞), and λ_o values were calculated from intercept and the slope of the linear region of the plots of $(n^2 - 1)^{-1}$ vs $(\lambda)^{-2}$ and are given in **Table 2**.

Rearranging of Equation (12), gives [36]

$$(n^2 - 1) = \frac{(S_o \lambda_o^2)}{1 - \left(\frac{\lambda_o}{\lambda}\right)^2} \tag{13}$$

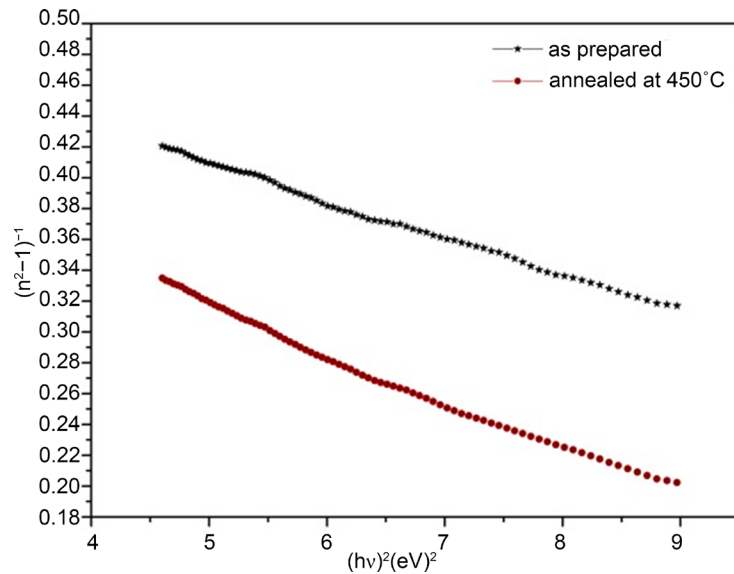


Figure 8. The plots of $(n^2 - 1)^{-1}$ versus $(hv)^2$ ZnO thin films.

where

$$S_o = (n_o^2 - 1) / \lambda_o^2 \quad (14)$$

The S_o values for ZnO films were obtained using above equation and are given in **Table 2**. The M_{-1} and M_{-3} moments of the imaginary part of the optical spectrum can be obtained from the relations [33]:

$$E_o^2 = \frac{M_{-1}}{M_{-3}}, E_d^2 = \frac{M_{-1}^3}{M_{-3}} \quad (15)$$

The M_{-1} and M_{-3} moments were calculated using Equation (15) and the obtained values are given in **Table 2**. The M_{-1} and M_{-3} moments changed due to the formation coordination of complex. It is found that M_{-1} and M_{-3} values increase with increase in annealing temperature.

3.4. Evaluation of Photocatalytic Activity

Figure 9(a), shows optical absorption spectrum of MB solution, before and after degradation under ZnO thin films. It revealed that the absorbance intensity of MB decreases obviously under visible light irradiation, which indicates that MB has been photodegraded. However, without light illumination, in the presence of ZnO film, and illumination in the absence of ZnO film does not result in the photocatalytic degradation of MB solution. A 200 W tungsten filament bulb was used as a light source. The standard solution of methylene blue with the concentration of 1×10^{-6} M was used as a model pollutant organic dye to determine the photocatalytic efficiency of the prepared photocatalyst. Photodegradation experiment was carried out by the ZnO film immersed into 15 ml of MB solution and it was stirred in the dark in order to reach adsorption-desorption equilibrium between MB and dissolved oxygen before irradiation and the beaker was kept in a chamber under visible light irradiation for different exposition times. Optical absorption spectrum of MB solution was measured using a UV-Vis spectrophotometer. The degradation efficiency was calculated using the following equation [37]

$$\text{degradation (\%)} = \frac{C_o - C}{C_o} \times 100 = \frac{A_o - A}{A_o} \times 100 \quad (16)$$

where C_o and C represent the initial concentration, after the adsorption-desorption equilibrium and at the reaction time (t) concentration of MB solution, respectively. A_o represents the initial absorbance, and A represents the changed absorbance of the MB solution at the characteristic absorption wavelength of 666 nm. The performance of degradation of as deposited and annealed ZnO films were reached to 90% and 93% after 240 min respectively. The highest catalytic activity was obtained by annealed ZnO catalyst due to the lower band gap energy. In addition, the relationship between the irradiation time and degradation reaction rate obeys the first-order reaction kinetic model, which could be well explained in terms of the Langmuir-Hinshelwood mechanism [37]. The kinetics can be expressed as

$$\ln\left(\frac{C}{C_0}\right) = -k_{app}t \quad (17)$$

where C and C_0 represent changed concentration and initial concentration of MB, k_{app} and t is the apparent rate kinetic constant and irradiation time, respectively. The plot of $-\ln\left(\frac{C}{C_0}\right)$ versus irradiation time (t) for ZnO is shown in **Figure 9(b)**.

Obtained kinetic plots are linear, which confirms that the photodegradation reaction of MB on ZnO is well fitted to the pseudo-first order reaction kinetics. The photocatalytic reaction rate constant (k_{app}) value for catalyst was estimated from the slop of this

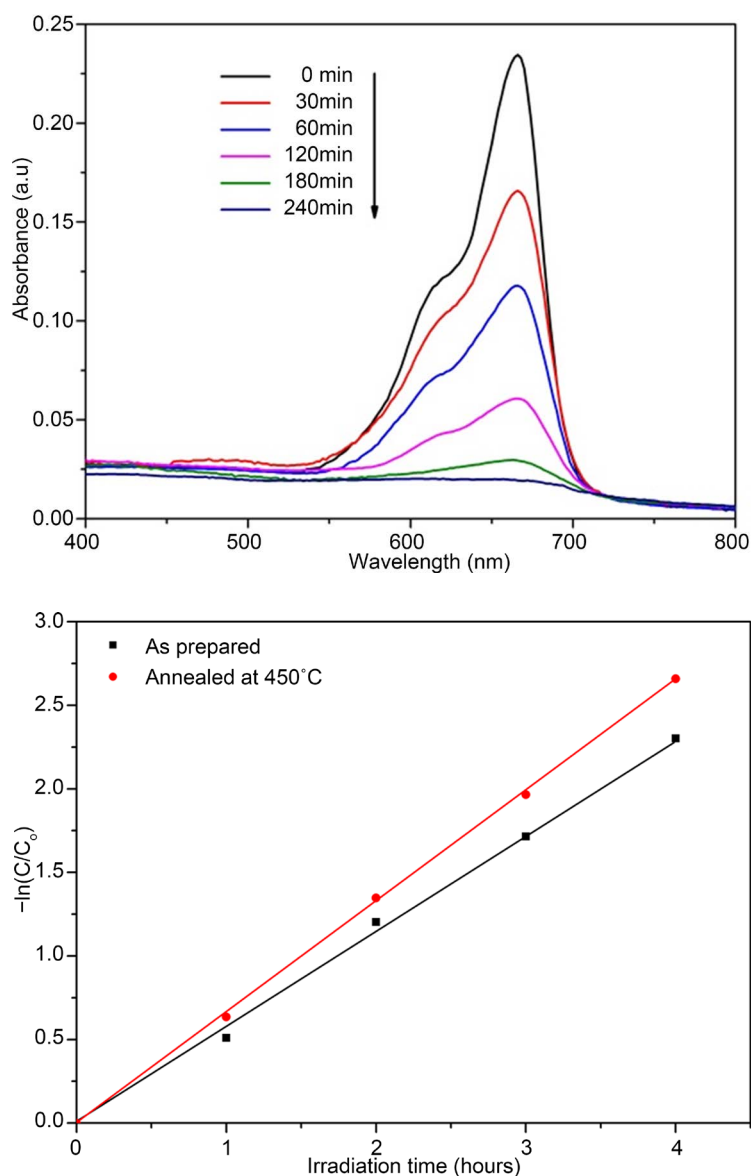


Figure 9. (a) Absorption spectra of MB catalyzed at room temperature in the presence of ZnO film annealed at 450°C, (b). The first order kinetics of the degradation of Methylene Blue dye with irradiation time.

linear plots and it were found to 0.0097 min^{-1} and 0.0111 min^{-1} for as deposited and annealed films respectively. It is clear that the catalytic activity higher for annealed ZnO. Therefore, the ZnO nanofibers with a low band gap can significantly increase the catalytic activity. However, the kinetic constant of the catalyst become smaller with greater band gap, because the opacity and light scattering of the ZnO nanofibers decrease the absorption of incident light and decrease catalytic active sites.

4. Conclusion

Visible light responsive zinc oxide films were deposited on glass substrate at a temperature of 350°C by chemical spray pyrolysis technique. The first order kinetic rate constant has been determined from the MB degradation measurement. ZnO film exhibits high catalytic activity for lower band gap energy. The lattice constants of hexagonal wurtzite structure ZnO films were calculated as 3.252 \AA and 5.204 \AA . Crystallite size has been found increase from 15 nm to 24 nm with annealing temperature. The SEM images of the films shown nano fiber like structure morphology and the average diameter of the fibers were $\sim 390 \text{ nm}$ and $\sim 400 \text{ nm}$ as deposited and annealed at 450°C respectively. The films exhibit low absorbance in the visible/near infrared (NIR) region from $\sim 390 \text{ nm}$ to 1000 nm . The direct optical band gap is 3.31 eV for deposited and 3.26 eV for annealed films. The oscillator energy (E_o), and the dispersion energy (E_d) of the ZnO thin films were determined. The values of oscillator energy (E_o) decrease, and the M_{-1} and M_{-3} optical moments increase with increasing annealing temperature. The long wavelength refractive index n_∞ , average inter band oscillator wavelength (λ_o) and the average oscillator length strength (S_o) parameters are found to be function of annealing temperature. The optical constants (refractive index n , extinction coefficient k , band gap energy and dielectric constant) of the as-deposited and annealed films were analyzed from the transmittance and reflectance spectra. Based on the observed data ZnO thin films are found to be a promising candidate for opto-electronic device and potential applications in the field of environmental remediation and photocatalysis.

Acknowledgements

One of the authors D. Komaraiah, thank the University Grants Commission, New Delhi for awarding the SRF, under the UGC scheme of RFSMS and also the authors R. Sayanna and M.V. Ramana Reddy, thank the UGC-UPE-FAR-OU for providing financial assistance to carry out this work.

References

- [1] Zhang, Y., Wu, C., Zheng, Y. and Guo, T. (2012) Synthesis and Efficient Field Emission Characteristics of Patterned ZnO Nanowires. *Journal of Semiconductors*, **33**, 023001. <http://dx.doi.org/10.1088/1674-4926/33/2/023001>
- [2] Song, J.Z., He, Y., Chen, J., Zhu, D., Pan, Z.D., Zhang, Y.F. and Wang, J.-A. (2012) Bicolor Light-Emitting Diode Based on Zinc Oxide Nanorod Arrays and Poly(2-Methoxy,5-Octoxy)-1,4-Phenylenevinylene. *Journal of Electronic Materials*, **41**, 431-436. <http://dx.doi.org/10.1007/s11664-011-1783-x>

- [3] Fortunato, E., Barquinha, P., Pimentel, A., Goncalves, A., Marques, A., Pereira, L. and Martins, R. (2005) Recent Advances in ZnO Transparent Thin Film Transistors. *Thin Solid Films*, **487**, 205-211. <http://dx.doi.org/10.1016/j.tsf.2005.01.066>
- [4] You, H.-C. (2013) Indium Doping Concentration Effects in the Fabrication of Zinc-Oxide Thin-Film Transistors. *International Journal of Electrochemical Science*, **8**, 9773-9784.
- [5] Suzuoki, Y., Ohki, A., Mizutani, T. and Ieda, M. (1987) Electrical Properties of ZnO-Bi₂O₃ Thin-Film Varistors. *Journal of Physics D: Applied Physics*, **20**, 511-517. <http://dx.doi.org/10.1088/0022-3727/20/4/017>
- [6] Müller, J., Rech, B., Springer, J. and Vanecek, M. (2004) TCO and Light Trapping in Silicon Thin Film Solar Cells. *Solar Energy*, **77**, 917-930. <http://dx.doi.org/10.1016/j.solener.2004.03.015>
- [7] Kim, D., Yun, I. and Kim, H. (2010) Fabrication of Rough Al Doped ZnO Films Deposited by Low Pressure Chemical Vapor Deposition for High Efficiency Thin Film Solar Cells. *Current Applied Physics*, **10**, S459-S462. <http://dx.doi.org/10.1016/j.cap.2010.02.030>
- [8] Faÿ, S., Steinhauser, J., Nicolay, S. and Ballif, C. (2010) Polycrystalline ZnO: B Grown by LPCVD as TCO for Thin Film Silicon Solar Cells. *Thin Solid Films*, **518**, 2961-2966. <http://dx.doi.org/10.1016/j.tsf.2009.09.189>
- [9] Badadhe, S.S. and Mulla, I.S. (2009) H₂S Gas Sensitive Indium-Doped ZnO Thin Films: Preparation and Characterization. *Sensors and Actuators B*, **143**, 164-170. <http://dx.doi.org/10.1016/j.snb.2009.08.056>
- [10] Kruefua, V., Liewhiranb, C., Wisitsoraatc, A. and Phanichphantd, S. (2011) Selectivity of Flame-Spray-Made Nb/ZnO Thick Films towards NO₂ Gas. *Sensors and Actuators B*, **156**, 360-367. <http://dx.doi.org/10.1016/j.snb.2011.04.046>
- [11] Shewale, P.S., Agawane, G.L., Shin, S.W., Moholkar, A.V., Lee, J.Y., Kim, J.H. and Uplane, M.D. (2013) Thickness Dependent H₂S Sensing Properties of Nanocrystalline ZnO Thin Films Derived by Advanced Spray Pyrolysis. *Sensors and Actuators B*, **177**, 695-702. <http://dx.doi.org/10.1016/j.snb.2012.11.076>
- [12] Dhawale, D.S., Dubal, D.P., More, A.M., Gujar, T.P. and Lokhande, C.D. (2010) Room Temperature Liquefied Petroleum Gas (LPG) Sensor. *Sensors and Actuators B*, **147**, 488-494. <http://dx.doi.org/10.1016/j.snb.2010.02.063>
- [13] Shinde, S.S., Bhosale, C.H. and Rajpure, K.Y. (2012) Photocatalytic Degradation of Toluene Using Sprayed N-Doped ZnO Thin Films in Aqueous Suspension. *Journal of Photochemistry and Photobiology B: Biology*, **113**, 70-77. <http://dx.doi.org/10.1016/j.jphotobiol.2012.05.008>
- [14] Kaneva, N., Stambolova, I., Blaskov, V., Dimitriev, Y., Bojinova, A. and Dushkin, C. (2012) A Comparative Study on the Photocatalytic Efficiency of ZnO Thin Films Prepared by Spray Pyrolysis and Sol-Gel Method. *Surface & Coatings Technology*, **207**, 5-10. <http://dx.doi.org/10.1016/j.surfcoat.2011.10.020>
- [15] Sahoo, T., Jang, L., Jeon, J., Kim, M., Kim, J., Lee, I., Kwak, J. and Lee, J. (2010) Photoluminescence Properties of ZnO Thin Films Grown by Using the Hydrothermal Technique. *Journal of the Korean Physical Society*, **56**, 809-812. <http://dx.doi.org/10.3938/jkps.56.809>
- [16] Gardeniers, J.G.E., Rittersma, Z.M. and Burger, G.J. (1998) Preferred Orientation and Piezoelectricity in Sputtered ZnO Films. *Journal of Applied Physics*, **83**, 7844-7854. <http://dx.doi.org/10.1063/1.367959>
- [17] Zhang, Y.A., *et al.* (2012) Synthesis and Efficient Field Emission Characteristics of Patterned ZnO Nanowires. *Journal of Semiconductors*, **33**, 023001. <http://dx.doi.org/10.1088/1674-4926/33/2/023001>

- [18] Taabouche, A., *et al.* (2013) Effect of Substrates on the Properties of ZnO Thin Films Grown by Pulsed Laser Deposition. *Advances in Materials Physics and Chemistry*, **3**, 209-213. <http://dx.doi.org/10.4236/ampc.2013.34031>
- [19] Lee, C.-H. and Kim, D.-W. (2013) Thickness Dependence of Microstructure and Properties of ZnO Thin Films Deposited by Metal-Organic Chemical Vapor Deposition Using Ultrasonic Nebulization. *Thin Solid Films*, **546**, 38-41. <http://dx.doi.org/10.1016/j.tsf.2013.05.029>
- [20] Saha, B., *et al.* (2014) Combined Effect of Oxygen Deficient Point Defects and Ni Doping in Radio Frequency Magnetron Sputtering Deposited ZnO Thin Films. *Thin Solid Films*, **562**, 37-42. <http://dx.doi.org/10.1016/j.tsf.2014.03.038>
- [21] Wang, H., Liao, C., Chueh, Y., Lai, C., Chen, L. and Tsiang, R.C. (2013) Synthesis and Characterization of ZnO/ZnMgO Multiple Quantum Wells by Molecular Beam Epitaxy. *Optical Materials Express*, **3**, 237-247. <http://dx.doi.org/10.1364/OME.3.000237>
- [22] Silva, T.G., Silveira, E., Ribeiro, E., Machado, K.D., Mattoso, N. and Hümmelgen, I.A. (2014) Structural and Optical Properties of ZnO Films Produced by a Modified Ultrasonic Spray Pyrolysis Technique. *Thin Solid Films*, **551**, 13-18. <http://dx.doi.org/10.1016/j.tsf.2013.11.011>
- [23] Hiltunen, L., Leskela, M., Makela, M. and Niinisto, L. (1987) Crystal Structure of μ_4 -Oxo-Hexakis (μ -Acetato) Tetrazinc and Thermal Studies of Its Precursor, Zinc Acetate Dihydrate. *Acta Chemica Scandinavica*, **41A**, 548-555. <http://dx.doi.org/10.3891/acta.chem.scand.41a-0548>
- [24] Cullity, B.D. (1987) Elements of X-Ray Diffraction. Addison-Wesley Publishing Company Inc., London.
- [25] Sridhar, R., Manoharan, C., Ramalingam, S., Dhanapandian, S. and Bououdina, M. (2014) Spectroscopic Study and Optical and Electrical Properties of Ti-Doped ZnO Thin Films by Spray Pyrolysis. *Spectrochimica Acta Part A: Molecular and Biomolecular Spectroscopy*, **120**, 297-303. <http://dx.doi.org/10.1016/j.saa.2013.09.149>
- [26] Ilicana, S., Caglara, Y., Caglara, M. and Yakuphanoglu, F. (2006) Electrical Conductivity, Optical and Structural Properties of Indium-Doped ZnO Nanofiber Thin Film Deposited by Spray Pyrolysis Method. *Physica E*, **35**, 131-138. <http://dx.doi.org/10.1016/j.physe.2006.07.009>
- [27] Maity, R., Das, S., Mitra, M.K. and Chattopadhyay, K.K. (2005) Synthesis and Characterization of ZnO Nano/Microfibers Thin Films by Catalyst Free Solution Route. *Physica E*, **25**, 605-612. <http://dx.doi.org/10.1016/j.physe.2004.09.002>
- [28] Willey, R.R. (1936) Field Guide to Optical Thin Films. SPIE Press, Bellingham.
- [29] Moss, T.S. (1961) Optical Properties of Solids. Butterworths, London, 34.
- [30] Tauc, J. (1974) Amorphous and Liquid Semiconductors. Springer, New York, Ch. 4. <http://dx.doi.org/10.1007/978-1-4615-8705-7>
- [31] Urbach, F. (1953) The Long-Wavelength Edge of Photographic Sensitivity and of the Electronic Absorption of Solids. *Physical Review*, **92**, 1324. <http://dx.doi.org/10.1103/PhysRev.92.1324>
- [32] Pankove, J.I. (1971) Optical Processes in Semiconductors. Dover, New York, 93.
- [33] Wemple, S.H. and DiDomenico Jr., M. (1971) Behavior of the Electronic Dielectric Constant in Covalent and Ionic Materials. *Physical Review B*, **3**, 1338-1351. <http://dx.doi.org/10.1103/PhysRevB.3.1338>
- [34] Wemple, S.H. (1972) Refractive-Index Behavior of Amorphous Semiconductors and Glasses. *Physical Review B*, **7**, 3767-3777. <http://dx.doi.org/10.1103/PhysRevB.7.3767>

- [35] Wolaton, A.K. and Moss, T.S. (1963) Determination of Refractive Index and Correlation to Effective Electron Mass in PbTe and PbSe. *Proceedings of the Royal Society*, **81**, 509.
<http://dx.doi.org/10.1088/0370-1328/81/3/319>
- [36] Lee, P.A., Said, G., Davis, R. and Lim, T.H. (1969) On the Optical Properties of Some Layer Compounds. *Journal of Physics and Chemistry of Solids*, **30**, 2719-2729.
[http://dx.doi.org/10.1016/0022-3697\(69\)90045-6](http://dx.doi.org/10.1016/0022-3697(69)90045-6)
- [37] Bizarro, M. and Martinez-Padilla, E. (2014) Visible Light Responsive Photocatalytic ZnO: Al Films Decorated with Ag Nanoparticles. *Thin Solid Films*, **553**, 179-183.
<http://dx.doi.org/10.1016/j.tsf.2013.10.059>



Scientific Research Publishing

Submit or recommend next manuscript to SCIRP and we will provide best service for you:

Accepting pre-submission inquiries through Email, Facebook, LinkedIn, Twitter, etc.

A wide selection of journals (inclusive of 9 subjects, more than 200 journals)

Providing 24-hour high-quality service

User-friendly online submission system

Fair and swift peer-review system

Efficient typesetting and proofreading procedure

Display of the result of downloads and visits, as well as the number of cited articles

Maximum dissemination of your research work

Submit your manuscript at: <http://papersubmission.scirp.org/>

Or contact mrc@scirp.org

